Indian Journal of Science and Technology, *Vol 9(44), DOI: 10.17485/ijst/2016/v9i44/101926, November 2016*
ISSN (Print) : 0974-6846
ISSN (Online) : 0974-5645

Modeling and Control of Low Frequency Dynamics of a Smart System

Mohit Kant*, Arti Motsara and Arun P. Parameswaran

Department of Electrical and Electronics Engineering, Manipal Institute of Technology, Manipal University, Manipal – 576104, Karnataka, India; mohitsahai12@gmail.com, artimotsara@yahoo.com, arun.p@manipal.edu,

Abstract

Background/Objectives: Active vibration control is an important aspect in mechatronic system dynamics and control. The objective of this manuscript is to present a classical PI controller in order to control the vibrations of a piezoelectric laminate flexible cantilever beam when excited by various signals. Methods/Statistical analysis: Finite element modeling techniques are employed to analytically develop the mathematical model of the smart system which replicates the low frequency system dynamics. The sensor, exciter and control actuator dynamics are modeled as well. The programming platform selected for developing the math model is MATLAB. The developed model was exported to SIMULINK platform for the controller design wherein classical PI control technique is implemented. **Findings:** The developed model is verified for its accuracy from its frequency response to free vibration condition which showed a close match between the resonant frequencies of the model with that derived from theory of vibrations. PI controller is the most commonly used controller worldwide due to its ease in computation as well as cost effectiveness. Its efficiency is proved in this manuscript when the system was subjected to free vibration in open loop as well as with the controller in loop. Further, as in practical cases, the system was also subjected to harmonic excitations at the dominant resonant frequencies and here as well, the controller was highly efficient in damping out the vibrations. **Application/Improvements:** The work presented in this manuscript can be extrapolated to any fixed-free system in aerospace, defence as well as heavy industries. The performance of the active controller can be further improved by opting for math intensive robust control strategies.

Keywords: Active Vibration Control, Modeling, Smart Systems, PI Controller

1. Introduction

Low frequency system noise and vibration is a persistent problem in a variety of light weight flexible structures such as flexible manipulators, flexible cantilever beams, and air craft's and space structures. Attractive field of application are slender structures with low natural damping like beams. Beam structure forms a basis for a lot of mechanical as well as electro-mechanical structures. Presently, inordinate advancement has been attained in the evolution of smart structures/systems accompanied with smart materials which serve as transducer as well as actuators. A smart structure deployed in the control of vibration can be described as a structure or structure's constituent with implanted or fused sensors and actuators accompanied by a control system, therefore, enabling the structure to react almost instantaneously to external excitation and then suppress unwanted effects or boost the desired effects[1]. Piezo ceramic materials form an important component of various smart systems due to their advantage over other smart materials because of their ease of implementation, cost-effectiveness, and lightweight. Large electromechanical coupling factor enables them to offer better sensing and actuation competencies that can further be employed for passive as well as active control of system dynamics[2,3].

**Author for correspondence*

Beam vibration can be classified along the flexural, lateral and torsional modes[4]. The Bending effect in a transversely vibrating beam was the single most significant parameter which was acknowledged by early researchers. The Euler-Bernoulli Beam model comprises the strain energy owing to its bending and the dynamic or kinetic energy due to the lateral displacement and the governing Euler-Bernoulli beam equation is grounded on the supposition that the plane perpendicular to the neutral axis before deformation rests orthogonal to the neutral axis after deformation[5]. A beam qualifies as an EB beam if its length to height ratio is greater than 10, and for low-frequency dynamics like vibrations, modeling of smart beam using EB theory is simple and provides reasonable engineering approximation[6].

In this work, a flexible aluminummaterial based cantilever beam was chosen which was further was smart by attaching patches of piezo electric smart material i.e. PZT-5H that served as transducer as well as actuators. The beam dynamics (vibration) defined by a 4th order PDE is modeled using the FE Theory and using a linear transformation, the SISO State space model for individual as well as multiple modes of vibration is developed[6–8]. The modeling was limited to a maximum of the third natural frequency for flexural mode vibrations as it has been proved that beyond the third natural frequency, the magnitude of vibrations is negligible and does not affect the dynamics of the system[9]. Prior to the parametric modeling, critical system parameters were determined via the non-parametric modeling procedure[9,10]. The obtained values of these critical system parameters were then used in the parametric modelling process to derive the final system models. The mathematical models were derived analytically for the primary resonance, secondary resonance, first two resonances as well as for a combination of the first three resonances in the flexural modes of vibrations. The derived models were then used to design classical industrial controllers based on the P, PI and PID technique[11]. The values were tuned so as to give a good control performance at the individual as well as a combination of flexural resonant regions.

2. Parametric Modeling of Piezoelectric Laminate Cantilever Beam

Consider a smart flexible aluminum cantilever beam sandwiched with piezoelectric patches at different finite element acting as sensors and actuators as shown in Figure 1. The beam is segregated into five finite elements as shown. A simple representation of a two node beam element + piezoelectric patch element is depicted in Figure 2 that highlighted the prominent degrees of freedom at each node points of the beam element. The sensors and actuators are bonded to 2nd element to sense as well as suppress the flexural mode of vibration while exciter patch is bonded to 4th Finite element. The beam is modeled using the following assumptions:

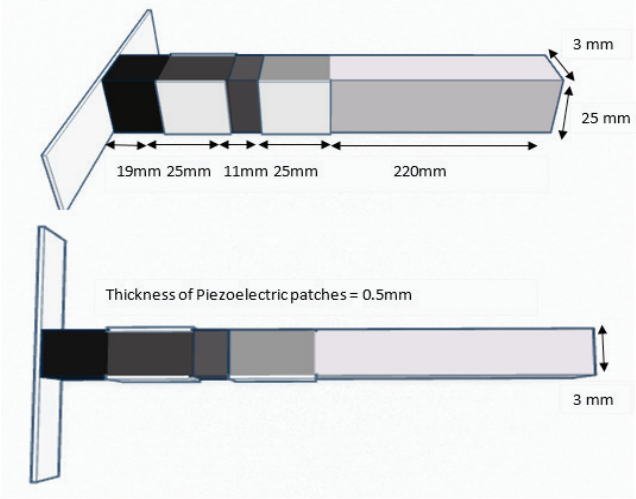

Figure 1. Piezoelectric laminate cantilever beam divided into five finite elements.

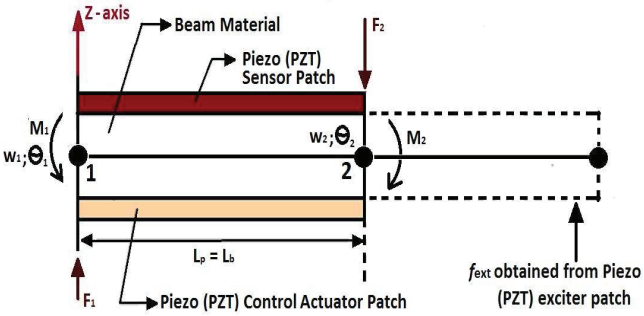

Figure 2. Schematic of a two node piezoelectric beam element

a) Cross-sections of the sensor, actuator ,and beam persist plane and orthogo0nal to the distorted longitudinal axis prior and later to bending. (Euler-Bernoulli theory)
b) Negligible contribution of the stiffness and mass of the adhesive material used in bonding Sensor, actuator as well as exciter of Smart beam element.
c) The piezoelectric material is homogeneous, transverse isotropic and elastic.

d) Neutral axis of the beam, sensor and actuator pass through the centroid.
e) The Effects of transverse shear forces of the sensor, actuator, and beam are ignored.
f) The beam component is supposed to exhibit 2 Degrees Of Freedom (DOF) at each node, viz., a transverse deflection *w* at the node and the spin angle or θ gradient at the node, which are called as the nodal variables. A bending moment actions at each individual nodal point corresponding to the two degrees of freedom at the individual node as shown in Figure 2.

The differential equation used to define the dynamics of the beam[12,13] is given as:

$$c^2\frac{\partial^4 w(x,t)}{\partial x^4}+\frac{\partial^2 w(x,t)}{\partial t^2}=0 \tag{1}$$

Where *w* is a multivariable variable function dependent typically on the local coordinate of the system measured from fixed end *x* and the time variable *t*. *w* depicts the transverse displacement of the beam.*c*is a constant dependent on various system parameters and is mathematically quantified by the expression given by $\sqrt{\frac{EI}{\rho A}}$. The critical system parameters *E*, *I*, ρ and *A* are modulus of elasticity, rotational inertia, compactness degree and cross sectional area of the beam respectively. The transverse displacement function *w (x,t)* appropriately describes the deflection behaviour of the beam element, which is obtained on solving (1). It is necessary that this displacement function satisfies the partial differential equation of equilibrium for the beam element. The solution of (1) is assumed as a third degree polynomial in the variable *x* and is given by

$$w(x,t)=a_1+a_2x+a_3x^2+a_4x^3 \tag{2}$$

The involved parameters in the expression (2) a_1, a_2, a_3 and a_4 are obtained by applying boundary condition at the nodal points of a beam element and are given by in matrix form as (3):

$$\begin{bmatrix}a_1\\a_2\\a_3\\a_4\end{bmatrix}\begin{bmatrix}a_1\\a_2\\a_3\\a_4\end{bmatrix}=\frac{1}{l_b^3}\begin{bmatrix}l_b^3 & 0 & 0 & 0\\0 & l_b^3 & 0 & 0\\-3l_b & -2l_b^2 & 3l_b & -l_b^2\\2 & l_b & -2 & l_b\end{bmatrix}\begin{bmatrix}w_1\\\theta_1\\w_2\\\theta_2\end{bmatrix}$$
$$\frac{1}{l_b^3}\begin{bmatrix}l_b^3 & 0 & 0 & 0\\0 & l_b^3 & 0 & 0\\-3l_b & -2l_b^2 & 3l_b & -l_b^2\\2 & l_b & -2 & l_b\end{bmatrix}\begin{bmatrix}w_1\\\theta_1\\w_2\\\theta_2\end{bmatrix} \tag{3}$$

where w_1, θ_1 and w_2, θ_2 are the Degree of freedom's at the fixed end node and free end node respectively and l_b is the length of the finite beam element. On substituting these values back into (2), the equation can be written in a matrix form as:

$$[W(x)]=[n^T][q] \tag{4}$$

Where n^T is a 1×4 matrix known as "shape function" and *q* is the vector of displacements and gradients (nodal displacement vector) and are described as

$$[n^T]=[f_1(x)\ f_2(x)\ f_3(x)\ f_4(x)] \tag{5}$$

and

$$n=\begin{bmatrix}1-3\frac{x^2}{l_b^2}+2\frac{x^3}{l_b^3}\\x-2\frac{x^2}{l_b}+\frac{x^3}{l_b^2}\\3\frac{x^2}{l_b^2}-2\frac{x^3}{l_b^3}\\-\frac{x^2}{l_b}+\frac{x^3}{l_b^2}\end{bmatrix} \tag{6}$$

$$q=\begin{bmatrix}w_1\\\theta_1\\w_2\\\theta_2\end{bmatrix} \tag{7}$$

The Lagrangian equation of a beam element with two nodes describes the transverse behaviour of regular beam element as

$$[M^b]=\rho_b A_b\int_0^{l_b}[n_2]^T[n_2]dx \tag{8}$$

$$[K^b]=E_b I_b\int_0^{l_b}[n_1]^T[n_1]dx \tag{9}$$

Where M^b and K^b are mass and stiffness matrices for a beam element and n_3, n_1 are the shape function and second derivative of the shape function respectively. Solution of (8) and (9), gives the elemental mass as well as elemental stiffness matrices and is obtained as:

$$M^b=\frac{\rho_b A_b l_b}{420}\begin{bmatrix}156 & 22l_b & 54 & -13l_b\\22l_b & 4l_b^2 & 13l_b & -3l_b^2\\54 & 13l_b & 156 & -22l_b\\-13l_b & -3l_b^2 & -22l_b & 4l_b^2\end{bmatrix} \tag{10}$$

$$K^b=\frac{E_b I_b}{l_b}\begin{bmatrix}\frac{12}{l_b^2} & \frac{6}{l_b} & -\frac{12}{l_b^2} & \frac{6}{l_b}\\\frac{6}{l_b} & 4 & -\frac{6}{l_b} & 2\\-\frac{12}{l_b^2} & -\frac{6}{l_b} & \frac{12}{l_b^2} & -\frac{6}{l_b}\\\frac{6}{l_b} & 2 & -\frac{6}{l_b} & 4\end{bmatrix} \tag{11}$$

In a similar fashion individual mass and stiffness matrices for piezoelectric patch can be defined using the (8) and (9) which depends on piezo patch density, area of cross section of piezopatch, length of piezo patch, Young's modulus and moment of inertia of piezo patch with respect to the neutral axis of the beam.

Similarly, for the beam element sandwiched between the piezo patches can be found out and similar results would be obtained[14]. But the constants attached to the mass and stiffness matrices would differ and are given as

$$EI = E_b I_b + 2E_p I_p \quad and \quad \rho A = b\left(\rho_b t_b + 2\rho_p t_a\right) \tag{12}$$

The moment rate is quantitatively measured by the output current of the piezo sensor. Implementation of a suitable smart structure instrumentation system (SSIS) with a pre-set signal conditioning gain (G_c) transforms the obtained output charge into an open circuit sensor voltage (V_{sensor}). The dynamic effect of sensor, actuator as well as exciter was also taken into account in the process of Finite Element Modeling in order to realize the overall dynamic equation of the smart system[15]. Finally, the State space model of the smart system was analytically derived using a linear transformation which incorporated the suitable amplifier gains and transformation matrices as shown in (13) and (14).

$$\begin{bmatrix} \dot{x}_1 \\ \dot{x}_2 \\ \dot{x}_3 \\ \dot{x}_4 \end{bmatrix} = \begin{bmatrix} 0 & I \\ -M^{*-1}K^* & -M^{*-1}C^* \end{bmatrix} \begin{bmatrix} x_1 \\ x_2 \\ x_3 \\ x_4 \end{bmatrix} + \begin{bmatrix} 0 \\ M^{*-1}T^T h \end{bmatrix} u(t) + \begin{bmatrix} 0 \\ M^{*-1}T^T f \end{bmatrix} r(t) \tag{13}$$

$$y(t) = \begin{bmatrix} 0 & p^T \end{bmatrix} \begin{bmatrix} x_1 \\ x_2 \\ x_3 \\ x_4 \end{bmatrix} \tag{14}$$

Where, M^* and K^* depicts the transformed global mass and stiffness matrices of the piezoelectric laminate flexible cantilever beam, C^*matrix depicts the structural damping of the system whereas T is the modal matrix used in linear transformation which contains the Eigen vectors depicting the preferred number of modes of vibrations of the smart system. The system mathematical models for the first, second and fourth natural frequencies were developed individually using the Finite Element Modeling techniques. Also the math models for the first two and first three flexural modes of vibration were developed. Finally, the state space model for first two vibratory modes is given as

$$\begin{aligned} \dot{x} &= Ax(t) + Bu(t) + Er(t) \\ y(t) &= C^T x(t) + Du(t) \end{aligned} \tag{15}$$

Where,

$$A = \begin{bmatrix} 0 & I \\ -M^{*-1}K^{-1} & -M^{*-1}C^* \end{bmatrix} \quad B = \begin{bmatrix} 0 \\ M^{*-1}T^T h \end{bmatrix}$$

$$C = \begin{bmatrix} 0 & -p^T T \end{bmatrix} \quad D = [0] \quad E = \begin{bmatrix} 0 \\ M^{*-1}T^T f \end{bmatrix}$$

The consistency of the derived math model was validated from its frequency response highlighting the dominant first natural frequency. An acceptable match between the observed first natural frequencies with that calculated from (16) proved the accuracy of the model. From the concept of machine vibrations, the natural frequency of the vibrating cantilever beam was determined as:

$$\omega_n = \sqrt{\frac{k}{m}} \tag{16}$$

Where, ω_n = the natural frequency of the beam (rad/sec)

$=2\pi f_n$

k = the beam stiffness (N/m^2)

m = the modal mass of the cantilever beam (Kg)

f_n = the natural frequency of the beam in Hz.

The dimensions of the system are as given in Table 1from which the beam cross section second area moment was determined by the following formula:

$$I = \frac{bh^3}{12} \tag{17}$$

Using (17) along with the known young's modulus (E) of the Aluminum based cantilever beam, the beam stiffness was calculated through the following formula:

$$k = \frac{3EI}{L^3} \tag{18}$$

From the free vibration test, the logarithmic decay ratio (δ) was determined as:

$$\delta = \frac{1}{n} \ln\left(\frac{X_n}{X_{n+1}}\right) \tag{19}$$

Also the logarithmic decay ratio can be formulized as:

$$\delta = \frac{2\pi\zeta}{\sqrt{1-\zeta^2}} \tag{20}$$

Further solution of (20) yielded the value for damping ratio (ζ) as:

$$\zeta = \frac{c}{c_c} = \frac{c}{2m\omega_n} = \frac{\delta}{\sqrt{4\pi^2 + \delta^2}} \tag{21}$$

Further simplification of (21) gives the relation for damping coefficient (c) as:

$$c = \frac{2\delta\sqrt{km}}{\sqrt{\delta^2 + 4\pi^2}} \quad (22)$$

Table 1. System parameters

Physical Parameters	Cantilever beam	Piezoelectric(PZT) sensor/actuator
Length	L_b = 300mm	L_p = 25mm
Width	b = 25mm	b = 25mm
Thickness	t_b = 3mm	t_p = .5mm
Density	ρ_b = 2700 Kg/m^3	ρ_p = 7700 Kg/m^3
Young's Modulus	E_b = 70GPa	E_p = 63GPa
Damping Constants used in C^*	α = 0.001 β = 0.0001	
PZT Strain Constant	----	d_{31} = -247x10-12 m/V
PZT Stress Constant	----	e_{31} = -9x10^{-3}Vm/N

3. Classical Control of the Low Frequency Dynamics - Simulations

The developed model was used in simulation studies to successfully design a classical PI controller that ensured a satisfactory servo and regulatory performance of the system dynamics. Figure 3 shows the schematic of controlled and uncontrolled system dynamics. The controller gains were suitably tuned such that the various control performance parameters like transient response, settling time, etc. were optimized when the models were subjected to a step input. Further, the performance of the designed controller was tested by subjecting the models to harmonic excitations at the individual dominant natural frequencies as well as in the first two vibratory modes which included the first two natural frequencies. For the controller gains of the time domain responses of the model are presented Figure 8-10. From the graphs, it is observed that the peak amplitude reduces by 51% while the settling time reduces by 27% for step response and the amplitude of oscillation reduces by 59% for harmonic response.

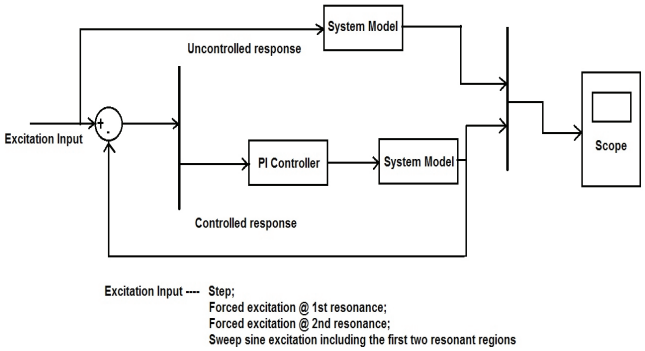

Figure 3. Overall schematic depicting the uncontrolled and controlled system dynamics

4. Results and Discussion

The frequency responses of the derived mathematical models were analysed to determine the dominant natural frequencies in the flexural mode of vibrations. Within the limitations on the system hardware, the computational intensity was raised by increasing the number of finite element. It was determined that with the increase in the finite elements, there existed a greater convergence in the values of the resonant frequencies to the accurate values. But, they came at a greater cost of increase in computational time as well as complexity. The effect of the number of finite element on the accuracy of the natural frequencies is tabulated in Table 2. Beyond 26 finite elements, it was not possible to execute the computation without the system crashing. The values of critical parameters were calculated using (16-22) and tabulated in Table 3 with the input excitation being a unit step signal whose time domain plots are shown in Figure 8. From Table 3, it was concluded that the best convergence possible was with 26 finite elements and the same was reflected in the corresponding frequency responses as shown in Figures 4–7. Time domain responses for harmonic excitation for first and second natural frequency are shown in Figures 9–10. The system model is also excited by a sweep sine signal for two different ranges of frequency to reduce the first and first two vibratory modes as shown in Figures 11–12.

Table 2. Convergence of frequency with increase in FE

Flexural Mode of Vibration	5 Finite Elements	14 Finite Elements	26 Finite Elements
1st	Fn1 = 30.6hz	Fn1 = 30.4hz	Fn1 = 26.4hz
2nd	Fn1 = 183hz	Fn1 = 174hz	Fn1 = 152hz
3rd	Fn1 = 618hz	Fn1 = 480hz	Fn1 = 417hz

Table 3. Critical system dynamics and their computed values.

Parameter	Formula	Value		Unit
First Natural Frequency	$f_n = \frac{1}{2\pi}\sqrt{\frac{k}{m}}$	**Analytical**	**Simulations**	Hz
		26.84	26.4	
Second Moment of area of the Beam cross section	$I = \frac{bh^3}{12}$	$5.625*10^{-11}$		m^4
Beam Stiffness	$k = \frac{3EI}{L^3}$	437.1		N/m
Logarithmic Decay	$\delta = \frac{1}{n}\ln\left(\frac{X_n}{X_{n+1}}\right)$	0.05162		--
Damping Coefficient	$c = \frac{2\delta\sqrt{km}}{\sqrt{\delta^2 + 4\pi^2}}$	0.0426		Ns/m

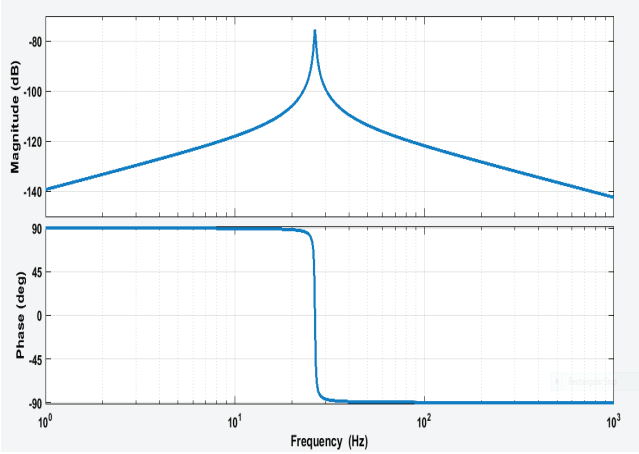

Figure 4. Bode plot projecting the first vibratory mode (Fn1)

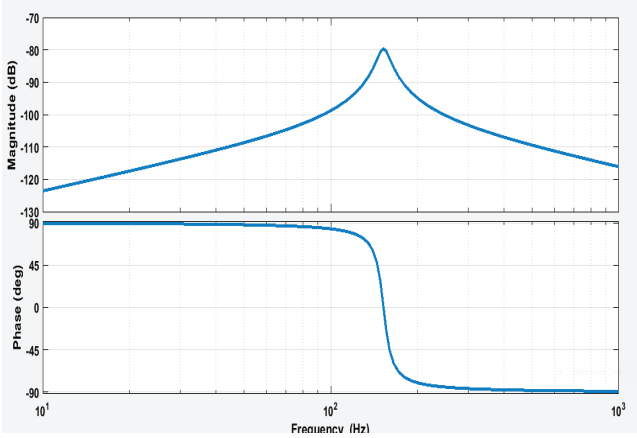

Figure 5. Bode plot projecting the second vibratory mode (Fn2)

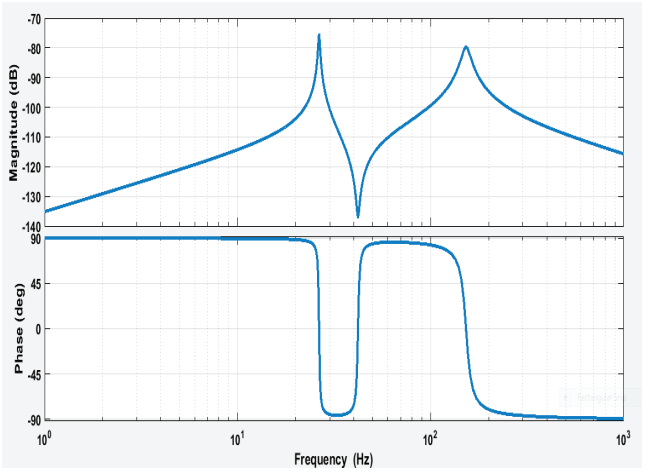

Figure 6. Bode plot projecting the first two vibratory modes (Fn1, Fn2)

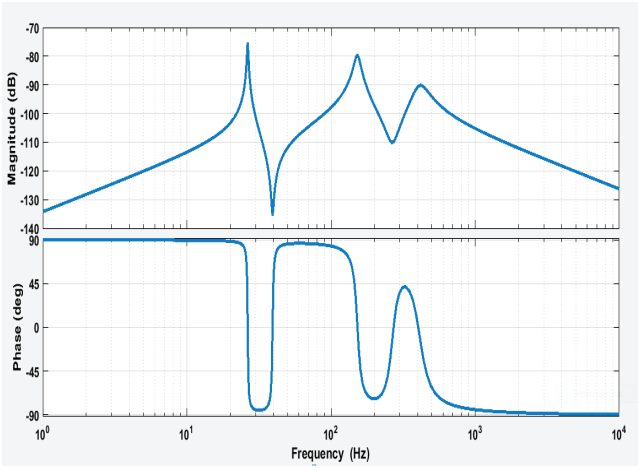

Figure 7. Bode plot projecting the first three vibratory modes (Fn1, Fn2, Fn3)

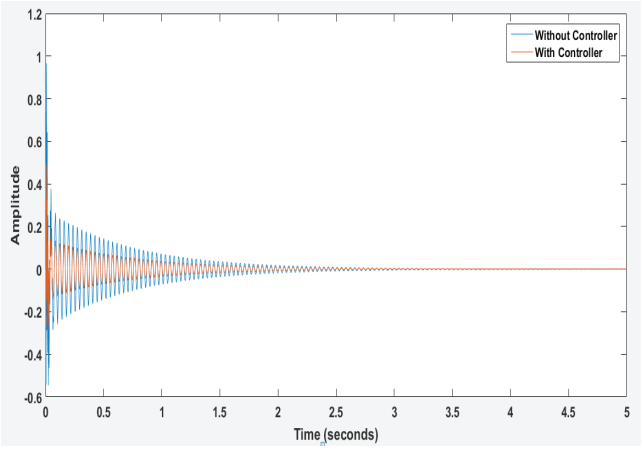

Figure 8. Step response of the model – uncontrolled and controlled

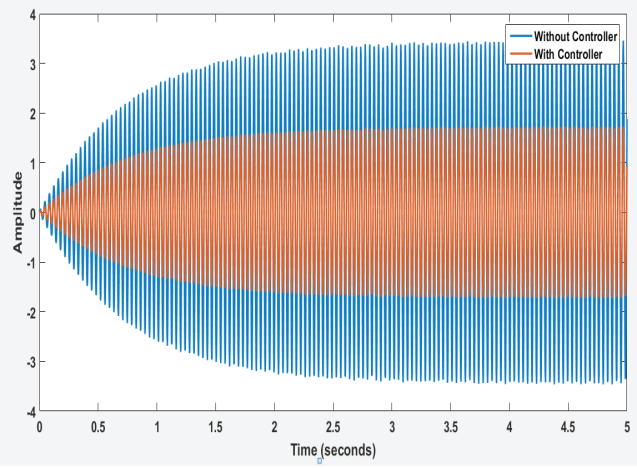

Figure 9. Forced excitation response for the first natural frequency

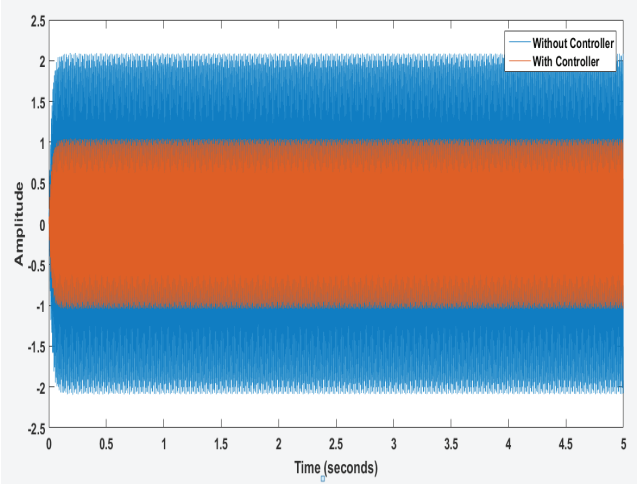

Figure 10. Forced excitation response for the second natural frequency

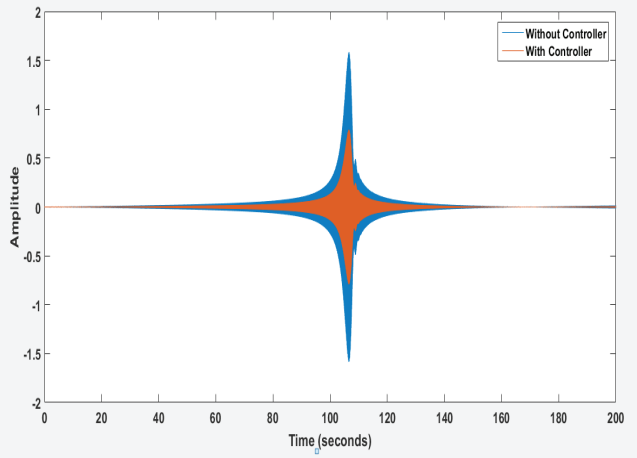

Figure 11. Sweep sine response for first vibratory mode

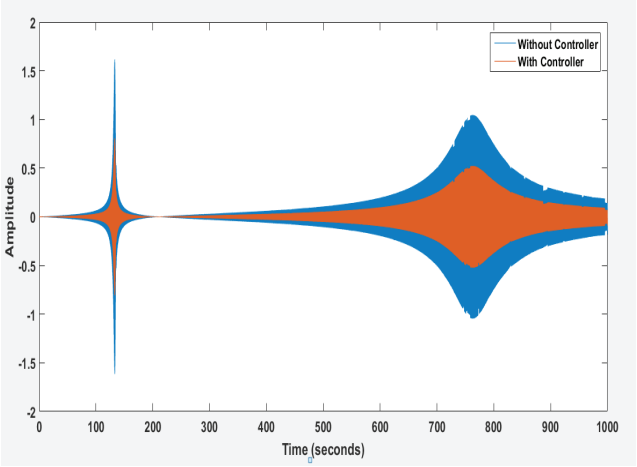

Figure 12. Sweep sine response for first two vibratory modes

5. Conclusion

In this work, the parametric modeling of a piezoelectric laminate cantilever beam for individual and multiple flexural modes of vibrations was performed. The dominant resonant frequency of the derived mathematical model was observed to be 26.4Hz as expected from theoretical calculations performed as a prerequisite via non-parametric modeling. At this frequency the system dynamics (vibration) tend to affect system the most in relation to its stability as well as operational efficiency. The convergence of frequencies in different vibratory modes was observed with an upsurge in the number of finite elements involved in system modeling. The frequency responses of the derived models highlighted the dominant natural frequencies in the flexural mode of vibrations. To control the dynamics, particularly at the resonant frequencies, a classical PI controller was designed and incorporated in the closed loop simulations. The controller was found to be successful in controlling the magnitude of the vibrations of the system in the individual resonances as well as the first two vibratory modes.

6. Future Scope

The hardware in loop studies will be performed on the system with the designed classical as well as future robust controllers in loop. The same will then be performed on a robotic arm so as to analyse its low frequency dynamics and perform their active control.

7. References

1. Xing JD, Guang M, Juan CP. Vibration Control of Piezoelectric Smart Structures Based on System Identification Technique: Numerical Simulation and Experimental Study, Journal of Sound and Vibration. 2006 Nov; 297(3-5):680–93.
2. Hurlebaus S, Gaul L. Smart Structure Dynamics, Mechanical Systems and Signal Processing. 2006 Feb; 20(2):255–81.
3. Song G, Sethi V, Li HN. Vibration Control of Civil Structures using Piezoceramic Smart Materials: A Review, Engineering Structures. 2006 Sep; 28(11):1513–24.
4. Annadurai A, Ravichandran A. Flexural Behavior of Hybrid Fiber Reinforced High Strength Concrete, Indian Journal of Science and Technology. 2016 Jan; 9(1):1–5. DOI: 10.17485/ijst/2016/v9i1/74084A.
5. Alhaza KA, Majeed MA. Free Vibration Control of a Cantilever Beam Using Combined Time Delay Feedback, Journal of Vibration and Control. 2012 Apr; 18(5):609–21.
6. Bandyopadhyay B, Manjunath TC, Umapathy M. Modeling, Control and Implementation of Smart Structures, 1st Editionn, Springer: Berlin, 2007.
7. Parameswaran AP, Gangadharan K. Parametric Modeling and FPGA Based Real Time Active Vibration Control of a Piezoelectric Laminate Cantilever Beam At Resonance, Journal of Vibration and Control. 2014 Jan; 21(14):2881–95.
8. Santa RK, Musalaiah G, Mohana KCK. Finite Element Analysis of a Four Wheeler Automobile Car Chassis, Indian Journal of Science and Technology. 2016 Jan; 9(2):1–5. DOI: 10.17485/ijst/2016/v9i2/83339.
9. Arun PP, Ananthakrishnan B, Gangadharan KV. Modeling and Design of Field Programmable Gate Array Based Real Time Robust Controller for Active Control of Vibrating Smart System, Journal of Sound and Vibration. 2015 Jun; 345:18–33. DOI: 10.1016/j.jsv.2015.02.002.
10. Arun PP, Ananthakrishnan B, Gangadharan KV. Design and Development of a Model Free Robust Controller for Active Control of Dominant Flexural Modes of Vibrations in a Smart System, Journal of Sound and Vibration. 2015 Oct; 355:1–18. DOI: 10.1016/j.jsv.2015.05.006.
11. Jaffar Sadiq Ali A, Ramesh G.P. Comparison of PI and PID Controlled Wind Generator Fed Γ- Z Source Based PMSM Drives, Indian Journal of Science and Technology. 2016 Jan; 9(1):1–6. DOI: 10.17485/ijst/2016/v9i1/71289.
12. Parameswaran AP, et.al. Active Vibration Control of a Smart Cantilever Beam on General Purpose Operating System, Defence Science Journal. 2013 Jul; 63(4):413–17.
13. Parameswaran AP, Gangadharan K. Active Vibration Control of a Smart Cantilever Beam at Resonance: A Comparison Between Conventional and Real Time Control. Proceedings of 12th International Conference on Intelligent Systems Design and Applications (ISDA), IEEE 2012, 235–39.
14. Fei J. Active Vibration Control of Flexible Steel Cantilever Beam using Piezoelectric Actuators. Proceedings of 37th South Eastern Symposium on System Theory, IEEE 2005, 35–39.
15. Hwang W, Park HC. Finite Element Modeling of Piezoelectric Sensors and Actuators, AIAA J. 1993 May; 31(5):930–37.